model with coupling over two cells requires almost twice as many input language statements for the circuit description. Further, the error due to the rather large cell size is the same in both models. The measured curve in Fig. 5 shows that the model predicts the measured impedance rather well. Since the accurate measurement of the low-impedance loop is difficult, three values have been averaged at each frequency point to improve confidence. Preliminary measurements on the same geometry with another conductor added, such that a U-shaped strip conductor results, showed an even larger inductance variation with frequency.

IV. CONCLUSIONS

The equivalent circuit model which has been presented is capable of predicting the inductance of nonstraight conductors as a function of frequency. When applied to corner-type geometries, the inductance was found to be much larger than for straight conductors assuming that both are close to a ground plane.

ACKNOWLEDGMENT

The authors wish to thank H. Lord who contributed to the project in its initial stages. Also, the helpful discussions with P. Grau are acknowledged.

REFERENCES

[1] R. W. Ilgenfritz, L. E. Mogey, and D. W. Walter, "A high density thick film multilayer process for LSI circuits," *IEEE Trans. Parts, Hybrids Packag.*, vol. PHP-10, pp. 165–168, Sept. 1974.
[2] V. A. Monaco and P. Tiberio, "Computer-aided analysis of microwave circuits," *IEEE Trans. Microwave Theory Tech. (Special Issue on Computer-Oriented Microwave Practices)*, vol. MTT-22, pp. 249–263, Mar. 1974.
[3] A. E. Ruehli, "Inductance calculations in a complex integrated circuit environment," *IBM J. Res. Develop.*, vol. 16, pp. 470–481, Sept. 1972.
[4] A. Gopinath and P. Silvester, "Calculation of inductance of finite-length strips and its variation with frequency," *IEEE Trans. Microwave Theory Tech.*, vol. MTT-21, pp. 380–386, June 1973.
[5] A. Gopinath and B. Easter, "Moment method of calculating discontinuity inductance of microstrip right-angled bends," *IEEE Trans. Microwave Theory Tech.* (Short Papers), vol. MTT-22, pp. 880–883, Oct. 1974.
[6] A. F. Thomson and A. Gopinath, "Calculation of microstrip discontinuity inductances," this issue, pp. 648–655.
[7] A. E. Ruehli, "Equivalent circuit models for three-dimensional multiconductor systems," *IEEE Trans. Microwave Theory Tech. (Special Issue on Computer-Oriented Microwave Practices)*, vol. MTT-22, pp. 216–221, Mar. 1974.
[8] W. T. Weeks *et al.*, "Algorithms for ASTAP—A network analysis program," *IEEE Trans. Circuit Theory (Special Issue on Computer-Aided Design)*, vol. CT-20, pp. 628–634, Nov. 1973.
[9] IBM Advanced Statistical Analysis Program, ASTAP Manual SH20-1118-0.

Prototype Characteristics for a Class of Dual-Mode Filters

ROBERT D. WANSELOW, SENIOR MEMBER, IEEE

***Abstract*—Selected prototype characteristics of nonequiripple antimetric elliptic-function filters which can be realized in orthogonal cascaded dual-mode circular or square waveguide structures are presented. Cavity-coupling data for 4-, 6-, and 8-section 0.01- and 0.05-dB-ripple passband designs with variable stopband levels are tabulated. Quantitative comparisons of elliptic and Chebyshev filter designs are also discussed, indicating the superior characteristics of elliptic networks.**

Manuscript September 26, 1974; revised February 24, 1975.
The author is with the TRW Systems Group, Redondo Beach, Calif. 90278.

INTRODUCTION

In recent years considerable emphasis has been placed on optimizing not only the electrical, but also the mechanical characteristics of narrow-band microwave communications waveguide bandpass filters. Near-optimum amplitude characteristics can be achieved utilizing elliptic functions which exhibit amplitude ripple in both the passband and stopbands [1]. However, the microwave realization of these near-optimum polynomials in the form of coupled cavities requires a departure from conventional cascaded synchronously tuned resonators [2] which exhibit a monotonically increasing stopband attenuation with or without a passband ripple response. That is, negative coupling must be available between predetermined sets of cavities. To achieve this, the hardware realization of such networks may make use of degenerate dual modes in single waveguide cavities, an idea which was first proposed by Ragan [3]. An added feature of the dual-mode cavity is the obvious reduction in size and weight.

In several excellent papers by Atia and Williams [4]–[7] the theory, together with experimental verification of various types of elliptic filters employing negative coupling in waveguide structures, has been well documented. The objective of this short paper is to present selected prototype parametric characteristics of antimetric elliptic-function filters which can be transformed into bandpass networks with emphasis directed toward cascaded dual-mode waveguide structures. Extensive tables of resonator coupling data for 4-, 6-, and 8-section filters have been developed as an aid for rapid design of these networks. All tabular data presented were generated from computer programs.

PROTOTYPE NETWORK CHARACTERISTICS

The equivalent circuit for N coupled cavities is shown in Fig. 1 which, for dual-mode operation, may include the additional terminal cross couplings indicated (M_{14} and $M_{N-3,N}$) and the M_{ij} coupling which exists for $N \geq 8$ sections, i.e., $M_{ij} = M_{36}$, where $(N = 8)$. Fig. 2 denotes the general orthogonal TE_{0n}-mode circular

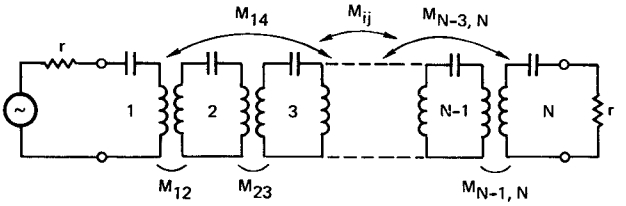

Fig. 1. Equivalent circuit of N coupled cavities (N = 4–8). Cross couplings available: $N = 4$: M_{14}; $N = 6$: $M_{14} = M_{36}$; $N = 8$: $M_{14} = M_{58}$, $M_{ij} = M_{36}$.

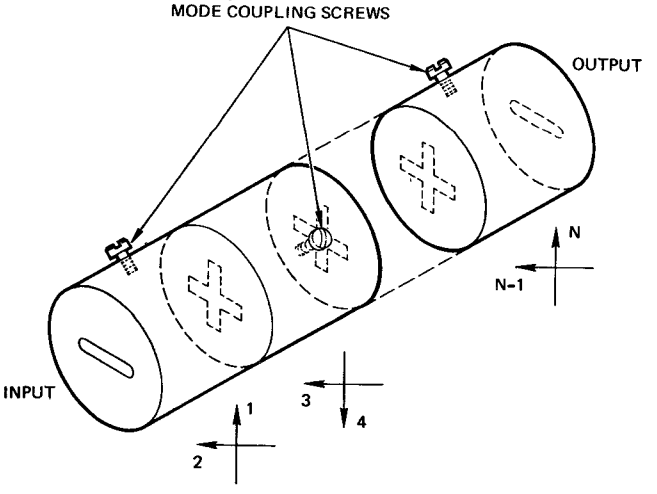

Fig. 2. Cascaded dual-mode circular-waveguide-cavity filter.

waveguide version of the circuit shown in Fig. 1. In square guide, the mode of operation is the TE_{101} rectangular mode.

The general low-pass characteristic transfer function can be written as $K(s) = \epsilon P(s)/Q(s)$ where ϵ is a constant and P and Q are monic polynomials in s. As the critical frequencies of the ratio $P(s)/Q(s)$ are changed in accordance with (2) in the Appendix, low-pass prototype response characteristics can be realized as shown in Fig. 3(a) and (b) for 4-, 6-, or 8-section filters. Thus, when the number of stopband transmission zeros (one of which is always at infinity) is less than $N - 2$, which is the case for $N > 4$, non-equiripple characteristics exist. Representative passband characteristics for 4-, 6-, and 8-section prototype filters are shown in Fig. 4. For all three curves, the number of stopband transmission zeros is two, as shown in Fig. 3(a) with $S_1 = 50$ dB and $R = 0.05$ dB, the common parameters. Thus two transmission zeros yield a single stopband lobe characteristics, and three zeros create the two-lobe response. Hence the numeral following the dash mark denotes the number of prototype stopband lobes. As N increases, the passband ripple match improves considerably as well as the obvious skirt sharpness (see Fig. 5).

Additional response characteristics of the prototype 8-section 2-transmission-lobe network are itemized in Table I for both 0.01- and 0.05-dB passband edge ripple levels. The maximum passband VSWR refers to the level of the highest reflection peak of the non-equiripple characteristics within the passband, excluding the skirt edge [see Fig. 3(b)].

Comparing a 10-pole Chebyshev filter with an $8 - 2$ elliptic network, each with the same passband ripple ($R = 0.05$ dB) normalized to the 50-dB stopband frequency, yields a Chebyshev bandwidth 96 percent that of the elliptic. Then, since the prototype zero-frequency time delays of each filter are 8.11 s (Chebyshev) and 4.39 s (elliptic, see Table II), the elliptic band-center loss would therefore be $(4.39/8.11) \times 0.96$, or 52 percent that of the Chebyshev filter, assuming each filter type has identical resonator unloaded Q's. If the required operating signal bandwidth was, say, 80 percent that of the elliptic passband, this would correspond to about 83 percent of the Chebyshev ripple bandwidth; then the corresponding time-delay ratios at $\omega' = 0.8$ would be 1.53 and 1.63, respectively, for the Chebyshev and elliptic responses. More importantly, from the loss-variation viewpoint, from $\omega' = 0$ to 0.8, the elliptic filter would be $(1.63/1.53) \times 0.52$, or about 56 percent that of the Chebyshev filter. Representative prototype time-delay characteristics for the class of elliptic function filters discussed are plotted in Fig. 6.

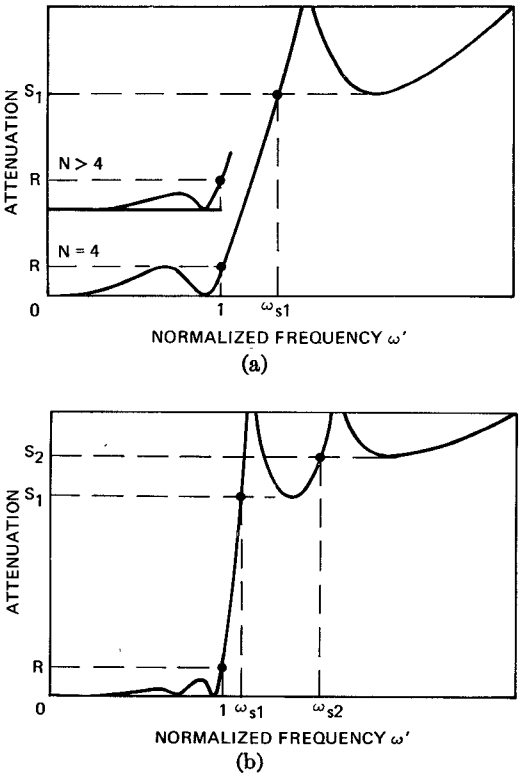

Fig. 3. Prototype antimetric elliptic-function responses. (a) Single-transmission-lobe response. (b) Double-transmission-lobe response of an 8-section filter ($N = 8 - 2$).

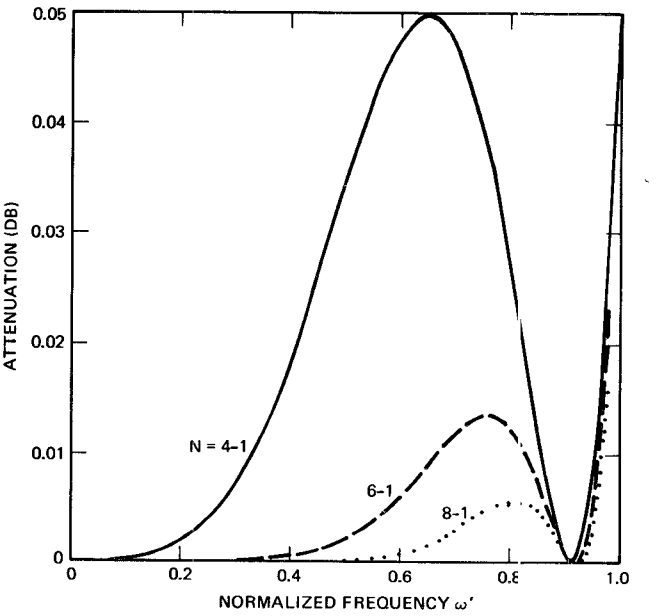

Fig. 4. Prototype single-transmission-lobe responses with $R = 0.05$ dB and $S_1 = 50$ dB.

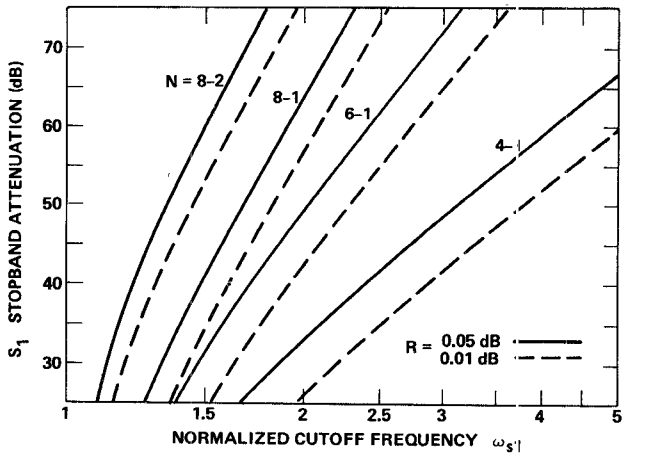

Fig. 5. Curves of stopband cutoff attenuation versus sharpness relative to the passband ripple edge frequency.

TABLE I
SOME PROTOTYPE PARAMETERS OF $N = 8 - 2$ FILTERS

	R = 0.01			R = 0.05		
S_1	ω_{s2}	S_2-S_1	Max Passband VSWR	ω_{s2}	S_2-S_1	Max Passband VSWR
70	2.382	9.084	1.074	2.168	8.938	1.181
60	2.084	8.861	1.076	1.901	8.668	1.186
50	1.828	8.562	1.080	1.674	8.296	1.190
40	1.614	8.173	1.081	1.484	7.807	1.192
30	1.434	7.642	1.083	1.326	7.166	1.202

TABLE II
PROTOTYPE ZERO-FREQUENCY TIME DELAY (SECONDS)

S_1 \ T_o	R = 0.01				R = 0.05			
	N = 4-1	6-1	8-1	8-2	4-1	6-1	8-1	8-2
70	1.797	2.921	4.056	4.452	2.154	3.295	4.438	4.807
60	1.779	2.877	3.992	4.296	2.129	3.236	4.364	4.624
50	1.747	2.811	3.908	4.090	2.086	3.158	4.265	4.387
40	1.691	2.716	3.796	3.832	2.010	3.042	4.133	4.085
30	1.593	2.579	3.646	3.502	1.880	2.877	3.961	3.709

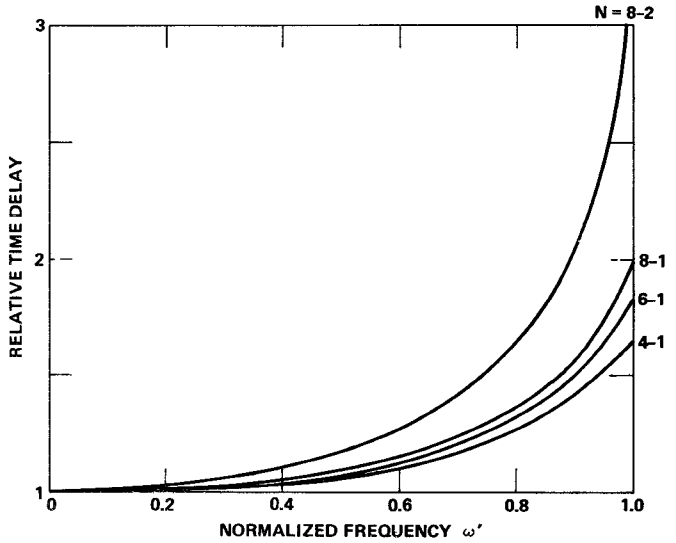

Fig. 6. Representative prototype time-delay characteristics for R = 0.05 dB and S_1 = 50 dB.

CAVITY COUPLING

The synthesis of the generalized two-port even-order network composed of synchronously tuned coupled cavities is given in [5], [6]. Upon reduction of the general even-mode coupling matrix to that of a practical solution for cascaded dual-mode circular waveguide cavities in which selected coupling terms have been eliminated, the remaining or modified coupling matrix was developed. Tables III and IV itemize these pertinent prototype mutual coupling M values for the circuits of Figs. 1 and 2. In addition, the loaded $Q(Q_e = 1/r)$ of the input and output coupling slots may be determined from the tabulated resistance r values. With reference to [8], coupling-slot dimensions for dual-mode waveguide bandpass filters can then be determined once the fractional bandwidth W is specified; that is, the prototype r and M values from Tables III or IV must be multiplied by W to yield the bandpass coupling parameters and external coupling values.

Since the filters studied are antimetric, only half of the M values are listed. That is, for $N = 4$: $M_{34} = M_{12}$; for $N = 6$: $M_{45} = M_{23}$, $M_{56} = M_{12}$, and $M_{36} = M_{14}$; for $N = 8$: $M_{56} = M_{34}$, $M_{67} = M_{23}$, $M_{78} = M_{12}$, and $M_{58} = M_{14}$. Coupling between modes within a single cavity is accomplished via the mode-coupling screws as indicated in Fig. 2. Thus, for all the filters, M_{12}, M_{34}, M_{56}, and M_{78} are realized by coupling screws, whereas all other coupling terms are realized in the form of long thin slots. The angular location of all mode-coupling screws is 45° with respect to either orthogonal cavity mode. However, the relative location of screws between adjacent cavities is determined by the sign of the cross-coupling terms M_{14}, M_{36}, and M_{58}.

CONCLUSIONS

Quantitative prototype data of even-order nonequiripple antimetric elliptic-function filters was given to aid the designer in making filter-response tradeoff analyses. Improved response characteristics of elliptic filters over conventional Chebyshev networks were discussed. Numerical data of cavity coupling applicable to cascaded dual-mode waveguide structures were also presented.

TABLE III
CAVITY COUPLING DATA FOR R = 0.01 dB

S_1	N	r	M = 12	23	34	45	14	36
70	4-1	1.59235	1.15162	0.84407			-0.02111	
	6-1	2.15709	1.36573	0.79709	0.69586		-0.03334	
	8-1	2.75927	1.66930	0.84622	0.68439	0.71167	0.02032	-0.07063
	8-2	2.00776	1.26457	0.65945	0.56397	0.82532	0.12364	-0.24268
60	4-1	1.58970	1.14794	0.84910			-0.03773	
	6-1	2.15493	1.36302	0.80195	0.68870		-0.04867	
	8-1	2.75819	1.66793	0.84455	0.68002	0.72670	0.02104	-0.09141
	8-2	2.00652	1.26033	0.65118	0.52551	0.88060	0.14397	-0.30549
50	4-1	1.58508	1.14113	0.85804			-0.06746	
	6-1	2.15159	1.35850	0.80948	0.67722		-0.07276	
	8-1	2.75668	1.66593	0.83410	0.67170	0.76389	0.04191	-0.13640
	8-2	2.00516	1.24997	0.63425	0.40467	0.99214	0.20786	-0.42253
40	4-1	1.57722	1.12811	0.87387			-0.12089	
	6-1	2.14673	1.35108	0.82059	0.65932		-0.10914	
	8-1	2.75456	1.66397	0.84070	0.65797	0.77623	0.01871	-0.16136
	8-2	2.00396	1.23853	0.63373	0.27037	1.06420	0.25273	-0.50593
30	4-1	1.56444	1.10184	0.90187			-0.21829	
	6-1	2.13979	1.33823	0.83718	0.63015		-0.16567	
	8-1	2.75169	1.66072	0.83667	0.63397	0.81899	0.01997	-0.22311
	8-2	2.00359	1.21490	0.65311	0.03267	1.10718	0.33989	-0.55869

TABLE IV
CAVITY COUPLING DATA FOR R = 0.05 dB

S_1	N	r	M = 12	23	34	45	14	36
70	4-1	1.21978	0.94161	0.73804			-0.01845	
	6-1	1.82409	1.17204	0.71104	0.63505		-0.02991	
	8-1	2.44603	1.48628	0.76356	0.62978	0.66633	0.01881	-0.06848
	8-2	1.71954	1.10348	0.60176	0.52109	0.79396	0.10427	-0.23993
60	4-1	1.21858	0.93889	0.74350			-0.03294	
	6-1	1.82380	1.17032	0.71677	0.62894		-0.04505	
	8-1	2.44695	1.48624	0.76445	0.62506	0.67877	0.01451	-0.08547
	8-2	1.72082	1.09978	0.59029	0.46360	0.86852	0.13485	-0.31952
50	4-1	1.21652	0.93378	0.75317			-0.05881	
	6-1	1.82344	1.16767	0.72460	0.62024		-0.06602	
	8-1	2.44823	1.48613	0.76278	0.61791	0.70127	0.01553	-0.11449
	8-2	1.72290	1.09385	0.58198	0.35926	0.95635	0.17486	-0.41359
40	4-1	1.21311	0.92375	0.77037			-0.10545	
	6-1	1.82300	1.16291	0.73666	0.60602		-0.09907	
	8-1	2.45008	1.48604	0.76116	0.60551	0.73181	0.01547	-0.15482
	8-2	1.72640	1.08365	0.58502	0.18365	1.03520	0.22988	-0.49974
30	4-1	1.20803	0.90273	0.80082			-0.19041	
	6-1	1.82276	1.15418	0.75469	0.58270		-0.15036	
	8-1	2.45294	1.48613	0.75965	0.58304	0.77412	0.01401	-0.21253
	8-2	1.73252	1.06320	0.61558	0.06488	1.05137	0.31428	-0.52284

APPENDIX

The general characteristic function $K(s)$ may be equated as follows

$$K(s) = \epsilon s^{N-2P} \prod_{v=1,3,\ldots}^{2P-1} \frac{(s^2 + a_v^2)}{(s^2 a_v^2 + 1)} \tag{1}$$

where the a_v terms are the critical frequencies. For N even, the critical frequencies are given by

$$a_v = (\sin\phi)^{1/2} \operatorname{sn}\left(\frac{vK}{2P+2}\right), \qquad v = 1,3,\cdots 2P-1 \tag{2}$$

where sn( ) is the Jacobian elliptic function with argument $(vK/2P + 2)$, K is the complete elliptic integral of the first kind, and the modular angle ϕ is related to the geometric mean of the passband and stopband bandwidths.

For even-order equal-ripple antimetric networks $2P = N - 2$, i.e., when the total number of transmission zeros is two less than the filter order. However, as the number of transmission zeros is reduced below this upper limit, both the passband return loss and stopband lobe structure will assume nonoptimum nonequiripple response characteristics as the critical frequency a_v distribution is changed in accordance with the modified argument of the Jacobian elliptic function in (2). Finally, the poles of the elliptic function filter are given as roots of the characteristic equation

$$1 + \epsilon^2 K(s)K(-s) = 0 \tag{3}$$

where only the left-half plane poles are utilized for network realization. The transmission zeros are determined from the roots of the denominator of (1) once the critical frequencies are known, and these are located symmetrically on the $j\omega$ axis.

REFERENCES

[1] S. Darlington, "Synthesis of reactance four poles which produce prescribed insertion loss characteristics," *J. Math. Phys.*, vol. 18, pp. 257–353, Sept. 1939.

[2] S. B. Cohn, "Direct-coupled-resonator filters," *Proc. IRE.*, vol. 45, pp. 187–196, Feb. 1957.

[3] G. L. Ragan, *Microwave Transmission Circuits*, vol. 9 (Rad. Lab. Series). New York: McGraw-Hill, 1948, pp. 673–677.

[4] A. E. Williams, "A four-cavity elliptic waveguide filter," *IEEE Trans. Microwave Theory Tech. (1970 Symp. Issue)*, vol. MTT-18, pp. 1109–1114, Dec. 1970.

[5] A. E. Atia and A. E. Williams, "New types of waveguide bandpass filters for satellite transponders," *COMSAT Tech. Rev*, vol. 1, pp. 21–43, Fall 1971.

[6] ——, "Narrow-bandpass waveguide filters," *IEEE Trans. Microwave Theory Tech.*, vol. MTT-20, pp. 258–265, Apr. 1972.

[7] ——, "Nonminimum-phase optimum-amplitude bandpass waveguide filters," *IEEE Trans. Microwave Theory Tech.*, vol. MTT-22, pp. 425–431, Apr. 1974.

[8] G. L. Matthaei, L. Young, and E. M. T. Jones, *Microwave Filters, Impedance-Matching Networks, and Coupling Structures*. New York: McGraw-Hill, 1964, pp. 229–243, 459–464.